IMPLICATIONS OF PROLONGED SOLAR MINIMUM CONDITIONS FOR THE SPACE DEBRIS POPULATION

Hugh G. Lewis[(1)] and Timothy Horbury[(2)]

[(1)] University of Southampton, Astronautics Research Group, Faculty of Engineering and the Environment, Southampton SO17 1BJ, United Kingdom, Email: hglewis@soton.ac.uk
[(2)] Imperial College London, Space and Atmospheric Physics Group, Department of Physics, Faculty of Natural Sciences, London SW7 2AZ, United Kingdom, Email: t.horbury@imperial.ac.uk

ABSTRACT

Observations of the current solar cycle show the likely continuation of a long-term decline in solar activity that began during the 1980s. This decline could lead to conditions similar to the Maunder minimum within 40 years [1], which would have consequences for the space debris environment. Solar activity is a key driver of atmospheric mass density and, subsequently, drag on orbiting spacecraft and debris. Whilst several studies have investigated potential effects on the global climate, no assessment has been made of the impact of a Maunder-like minimum on the space debris population in Low Earth Orbit (LEO). Consequently, we present a new study of the future debris environment under Maunder minimum conditions and provide an assessment of the possible consequences to the LEO space debris population and space operations.

The University of Southampton's Debris Analysis and Monitoring Architecture to the Geosynchronous Environment (DAMAGE) has been used to analyse the consequences of a Maunder minimum of approximately 50 years duration and to quantify the impact on the effectiveness of debris mitigation measures. Results from these studies suggest an increase in collision activity and a corresponding, rapid growth of the debris population during a Maunder minimum period, in spite of on-going mitigation efforts. In the best case, the DAMAGE results suggest that the population of debris > 10 cm could double in number by the end of Maunder minimum conditions. However, the rapid growth in the population is followed by a strong recovery period on exit from a Maunder minimum. The recovery is characterised by a decrease in the debris population, which can be to a level similar to that seen before the onset of the Maunder minimum, if mitigation efforts are sustained. As such, prolonged solar minimum conditions may have relatively benign implications for the long-term evolution of the debris environment. However, the risks to spacecraft from collisions with debris during a Maunder-like minimum would be considerably higher than present, and exacerbated by any deficiency in debris mitigation efforts, with corresponding impacts on space operations.

1 INTRODUCTION

The familiar solar sunspot cycle is a manifestation of a dynamo in the Sun's interior, with the solar magnetic field effectively flipping every 11 years. Low sunspot numbers – solar minimum – occur when the global field is relatively dipolar-like, while solar maximum corresponds to a much more complex and variable field configuration.

Since the earliest systematic sunspot observations in the seventeenth century, it has become clear that the sunspot cycle is itself variable, both in period and amplitude (Fig. 1). The most celebrated change in the cycle is the Maunder minimum, from around 1645 to 1700, when very few sunspots were observed. The weaker Dalton minimum, from around 1790 to 1830, comprised a set of cycles with sunspot maxima significantly lower than those around them.

More recently, approximately coinciding with the start of the Space Age, the Sun entered a period of enhanced activity known as a Grand Solar Maximum. Since the mid-1980's, however, activity levels have reduced. The minimum before the start of the current Cycle 24 was longer than expected and as the sun approaches its maximum, the cycle is much weaker than those immediately preceding it, suggesting a continued decline (see [1] for a recent review). Indeed, there is some evidence from helioseismology measurements (e.g. [2]) that precursors of the next cycle within the solar interior are also weaker than at this point in the cycle, suggesting that Cycle 25 might be weaker again.

Solar cycle changes in its magnetic field have effects elsewhere, for example in modulating the cosmic ray flux at the Earth as a result of alterations in the interplanetary magnetic field. This makes it possible to use secondary measurements, such as cosmogenic isotope production, to extend estimates of solar activity levels beyond the earliest systematic sunspot observations. Such reconstructions show that solar activity levels are indeed variable over a range of scales, that the Sun can enter an extended period of low activity, such as the Maunder minimum, after a Grand Solar Maximum and that this occurs after around 1 in 10 of such maxima [3].

Proc. '6th European Conference on Space Debris'
Darmstadt, Germany, 22–25 April 2013 (ESA SP-723, August 2013)

It is therefore unlikely but not impossible that the Sun is in the process of entering a low activity state, similar to the Maunder or Dalton minima. If such a change, unprecedented since the beginning of the Space Age, were to occur, it would have significant effects on the space environment of the Earth and near-Earth space, for example in enhanced cosmic ray flux. It would also reduce the F10.7 EUV flux incident on the Earth's atmosphere, and through lowered heating rates reduce drag on objects in Low Earth Orbit. Such a reduction in drag could increase the orbital debris population and hence increase the risk to operational assets.

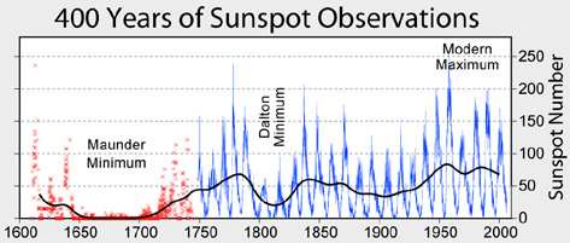

Figure 1. 400 years of Sunspot observations (Image created by Robert A. Rohde, Global Warming Art, http://www.globalwarmingart.com/wiki/File:Sunspot_Numbers_png).

2 THE DAMAGE MODEL

The Debris Analysis and Monitoring Architecture to the Geosynchronous Environment (DAMAGE) is a three-dimensional computational model of the full LEO to GEO debris environment. It includes source models for objects down to 10 cm but is capable of evolving populations of objects down to 1 mm.

DAMAGE is supported by a fast, semi-analytical orbital propagator, a breakup model, several collision prediction algorithms including a method based on the CUBE approach adopted in NASA's LEO-to-GEO Environment Debris model (LEGEND) [4], and a satellite failure model, which accounts for mission failures resulting from the non-catastrophic impacts of small particles. Projections into the future are typically performed using a Monte Carlo (MC) approach to account for stochastic elements within the model and to establish reliable statistics.

2.1 DAMAGE Orbital Propagator

The DAMAGE orbital propagator includes orbital perturbations due to Earth gravity harmonics (J2, J3, and J2,2), luni-solar gravitational perturbations, solar radiation pressure and atmospheric drag. The drag model assumes a rotating, oblate atmosphere with high-altitude winds. Atmospheric density and density scale height values are taken from the 1972 COSPAR International Reference Atmosphere (CIRA), which includes semi-annual and diurnal variations.

Atmospheric decay remains the only effective sink mechanism for space debris up to altitudes of about 600 km. The drag acceleration, a_D, on a satellite with cross-sectional area A and mass M is a linear function of the local mass density, ρ,

$$a_D = \frac{1}{2}\frac{A}{M} C_D \rho v_r^2, \quad (1)$$

where C_D is the drag coefficient and v_r is the velocity of the satellite relative to the atmosphere. A decrease in mass density will, thus, produce a corresponding decrease in the drag acceleration on a satellite, leading to an increase in the orbital lifetime.

Solar irradiance is a key driver of mass density change in the thermosphere. Changes in solar irradiance over the 11 year solar cycle cause corresponding mass density changes of up to an order of magnitude [5]. These changes in density cause large variations in atmospheric drag, from (1), and the rate at which orbiting objects re-enter the atmosphere.

In DAMAGE, the total mass density and density scale height are stored as look-up tables for discrete altitudes and exospheric temperatures. Log linear interpolation is used to extract density and scale height estimates from the look-up tables at the perigees of all objects within the LEO region for $F_{10.7}(t)$ values throughout the projection period. The exospheric temperature, $T_{ex}(t)$, at time t is

$$T_{ex}(t) = 1.125\left(379 + \left[3.24 F_{10.7}(t)\right]\right) + 59.89 + \Delta T_{ex}(t), \quad (2)$$

where $F_{10.7}(t)$ is the solar flux at a wavelength of 10.7 cm and $\Delta T_{ex}(t)$ is a correction factor for the semi-annual variability. The constant (59.89) is a correction due for geomagnetic activity, which is based on a 20-year average represented by K_p = 2.13. Projected solar activity is described in DAMAGE typically using a pseudo-sinusoidal model, but has been modified for this work to account for a prolonged period of low solar activity.

2.2 DAMAGE Collision Probability Estimation

DAMAGE normally uses an approach based on NASA's CUBE algorithm [6] for predicting collision risk. The advantage of this approach is that it involves a simple calculation and scales linearly with the number of objects. Whilst the implementation developed by NASA assumes a non-zero collision probability only for objects residing within the same "cube", the DAMAGE algorithm ensures that all close approaches within a user-specified distance from a target are identified and analysed. This is achieved, essentially, by calculating the position of the target and the debris in a geo-centric Cartesian coordinate system and then by "binning" the values in the x-, y- and z-directions. The aim is then to

identify all cases where a target spacecraft and a debris particle reside in the same cube bin [6]. By expanding the search to include cases where a target spacecraft and debris reside in neighbouring cubes – in Cartesian space, there are eight neighbouring cubes – and then applying a distance constraint, the DAMAGE approach identifies all cases where a target spacecraft and a debris particle could reside in a cube of a specified size and any orientation (see Fig. 2). For this work, the bin (cube) size was set to 10 km resulting, through use of the Pythagoras theorem, in the identification of conjunctions with a maximum separation with respect to the target spacecraft of 17 km.

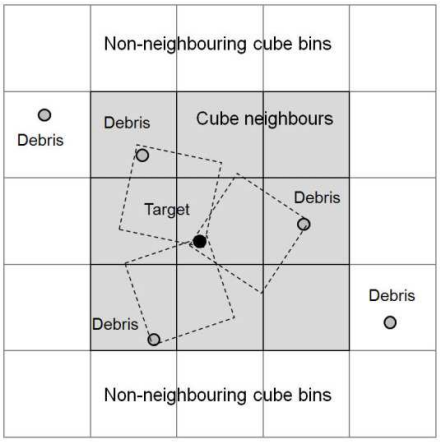

Figure 2. Two-dimensional representation of the Kernel approach in DAMAGE. By including cubes that are near-neighbours in its search and applying a distance constraint (the maximum distance is ~17 km), the method identifies all debris particles that could reside with the target spacecraft in a cube of side 10 km and in any orientation.

This approach takes no account of the movement of the target spacecraft or the debris within a time-step. That is, only the instantaneous positions of the objects are used in the cube-binning process; this results in a "snapshot" of the collision risk and not a true estimate of the risk over time. The original CUBE method (used for long-term projections) generates better estimates of the collision risk though a "sampling in time" approach, whereby the collision risk is accumulated over many snapshots and over a long projection period.

The collision probability of a target spacecraft with a debris object in the same cube volume element dU over the time-step dt is,

$$P_{col} = \frac{|\mathbf{v_R}| \sigma \, dt}{dU}, \tag{3}$$

where $\mathbf{v_R}$ is the relative velocity of the debris particle relative to the target spacecraft, and σ is the combined cross-sectional area of both objects. Here, σ is

$$\sigma = S_T + S_D + 2\sqrt{S_T S_D} \tag{4}$$

for a target area, S_T, and a debris area, S_D, assuming both objects to be spherical. The calculation of collision probability assumes that the target object can reside at any point within the cube volume with uniform probability.

3 METHOD

A 200-year future projection of the LEO space debris population $\geq$ 10 cm from 1 May 2009 was used by DAMAGE as the benchmark (normal) scenario for this investigation. The initial population was taken from the MASTER 2009 population of space debris and included all objects $\geq$ 10 cm intersecting the LEO region. It was assumed that future launch traffic could be approximated by repeating the 2001-2009 launch cycle.

The benchmark scenario incorporated key elements of the IADC space debris mitigation guidelines, including post-mission disposal (PMD) to limit the lifetime of spacecraft and launch vehicle orbital stages in the LEO region. These objects were moved to 25 year decay orbits or LEO storage orbits (above LEO) depending on the delta-v. As the storage orbits were above LEO, objects placed here were no longer processed in the simulation. PMD measures were implemented from the start of the future projection and were applied to 90% of all eligible objects. In addition to the PMD measures, it was assumed that no explosive breakups occurred in the projection period.

The benchmark scenario was modified to account for different future solar activity, the addition of Active Debris Removal (ADR) and to account for the effects of a secular change in the thermospheric mass density (Tab. 1). The changes made to the benchmark scenario are described in detail in the following sections. The analyses of each scenario (except where indicated) were based on the results of 100 Monte Carlo (MC) runs.

Table 1. Description of DAMAGE scenarios.

Scenario	Description
Normal	Normal pseudo-sinusoidal solar activity model, PMD and no explosions
Maunder-like	As normal but with constant, low solar activity from 2020 through 2065, followed by weak cycle
Dalton-like	As normal but with repeated weak cycles from 2020 through 2065
Maunder-like with ADR	As Maunder-like but with the removal of three objects per year, starting in 2020, according to removal criterion (5)
Maunder-like with density trend	As Maunder-like but with future atmospheric mass density decline, according to (6). 40 MC runs

3.1 Future Solar Activity

A pseudo-sinusoidal model was used to represent future solar activity in the benchmark scenario. This model was modified to include a period of low solar activity persisting for approximately 65 years. For the Maunder-like case, the lowest solar flux from Cycle 23 was used for this period. The first cycle after the Maunder-like period was assumed to be a repeat of the weak Cycle 24. In addition, a Dalton-like case was generated by repeating Cycle 24 over the 2020-2065 period. The resulting solar activity cases are shown in Fig. 3.

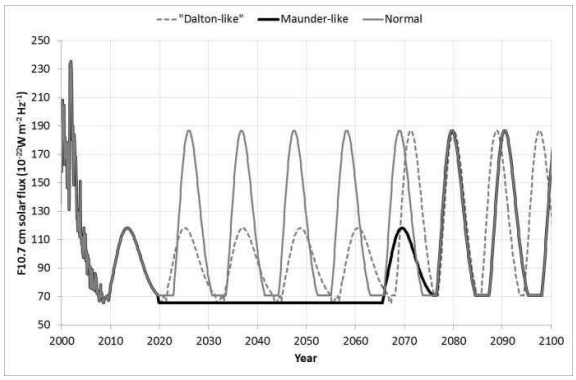

Figure 3. Future solar activity (F10.7 cm solar flux) cases.

3.2 Active Debris Removal

Objects were targeted for removal based on their probable contribution to future collision activities. Thus, the probability of an object being involved in a collision, and the likely number of fragments added to the environment if a collision does occur, were used to define the criterion [15]

$$R_i(t) = m_i \sum_{j \neq i} P_{i,j}(t) \tag{5}$$

to rank objects for removal. Here m_i is the mass of object i, which is a key factor in the NASA standard breakup model for determining the number of collision-induced fragments [16]. The estimation of the cumulative probability $\sum P_{i,j}(t)$ over all objects $j \neq i$ for use in this removal criterion was made outside the normal environment projection in DAMAGE and was achieved using an integration of (3) over a relatively short time interval (days), at the start of each ADR year.

In addition, the following eligibility requirements for removal were used.

1. The object must be intact (i.e., a payload, launch vehicle upper stage or mission-related debris).
2. The object must have an orbital eccentricity <0.5.
3. The object must have a perigee altitude <1400 km.

The object must not already be subject to PMD measures.

3.3 Future Mass Density Changes

In addition to the effects of solar irradiance, temperature changes in the mesosphere and lower thermosphere (60–100 km altitude) are also caused by the excitation of atmospheric CO_2 by collisions with atomic oxygen, which result in infrared emission at 15 μm and a net cooling [7]. The anticipated doubling of the concentration of CO_2 by the end of the 21st century may lead to a cooling of 10 K in the thermosphere, increasing to 50 K in the mesosphere [8], and a corresponding decrease in mass density at higher altitudes.

Empirical studies of thermospheric mass density change using satellite drag data have been performed by [9], [10], [11] and [12]. In general, these studies derive total mass densities, or changes in total mass densities, from a subset of the Two-Line Element (TLE) catalogue generated by the U.S. Space Surveillance Network. Findings from these studies suggest an overall thermospheric density trend in the range −2% to −5% per decade. The secular nature could lead to a reduction in thermospheric density to half of the present value within 100 years at a given height if CO_2 concentrations increase as expected [10]. The density reduction will lead to increasing lifetimes for satellites and space debris. Simulations of the space debris environment have shown that these effects augment the collision rate, increase the number of objects ≥ 10 cm [13], and decrease the effectiveness of debris mitigation and remediation efforts [14].

Following the approach adopted by [13] and [14], DAMAGE accounts for thermospheric cooling using an empirically derived secular density change. Here, the empirical model was developed from 30 satellites in LEO [12]; the modified density,

$$\rho_c = \rho_i \left[(0.98028 - 0.00013h)^T (0.00109 F_{10.7}(t) + 0.88578) \right] \tag{6}$$

at height h and for 10.7 cm solar flux, is estimated from the initial density, ρ_i, obtained using log-linear interpolation of the CIRA-72 density values stored in the DAMAGE look-up table, and at time T measured in decades from the epoch 1 January 1970.

4 RESULTS

The effective number of objects in LEO over the projection period for the benchmark (normal) mitigation and the Maunder-like scenarios are shown in Fig. 4. The 1-sigma standard deviations for each scenario are also shown. For purposes of clarity, these 1-sigma values are

omitted from the remaining figures.

Fig. 4 shows a nearly linear growth in debris population during the Maunder-like minimum period, even with good compliance with recognised debris mitigation measures. In fact, the population grows at a rate of ~250 objects per year during this period, compared with a slight decrease in the population under normal solar activity over the same time period. By 2075, DAMAGE predicts 29,205 objects ≥ 10 cm in LEO, an increase of 70.7% from the 2009 population. However, once normal solar activity resumes, the LEO population decreases relatively quickly to ~22,500 by 2120 and subsequently remains relatively constant to the end of the projection period; an increase of 31.5% compared with the 2009 population and only 12.5% higher than the population predicted for 2209 under normal solar activity.

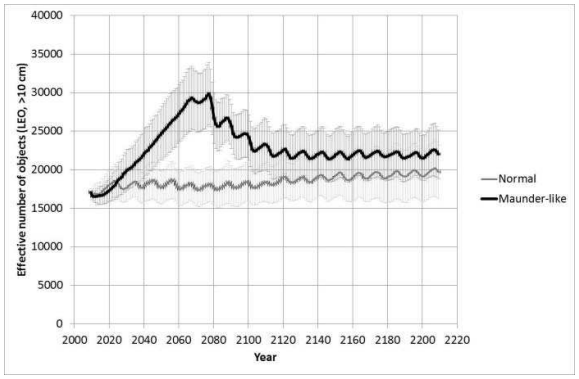

Figure 4. Effective number of objects≥ 10 cm in LEO, and 1-sigma standard deviations, for the normal and Maunder-like scenarios.

Fig. 4 also suggests that the LEO population is stable or, even, asymptotically stable as the populations in both the normal and Maunder-like scenarios seem to converge to an equilibrium. This is more readily apparent in Fig. 5, which shows the effective number of objects ≥ 10 cm in LEO for all of the scenarios.

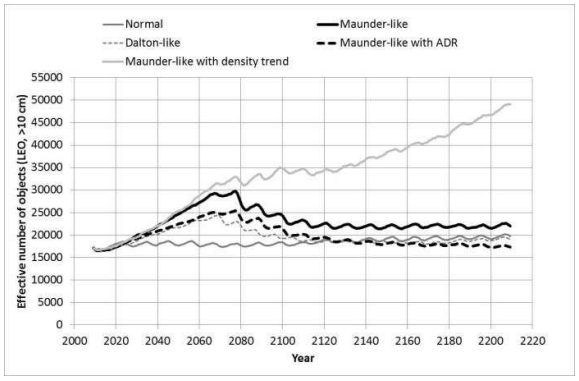

Figure 5. Effective number of objects≥ 10 cm in LEO, for each DAMAGE scenario.

For the Normal, Maunder-like and Dalton-like scenarios, the LEO population converges to a mean of 20,530 (± 1612) objects, in spite of large excursions in population size during the simulated prolonged solar minimum period between 2020 and 2065.

The cumulative number of catastrophic collisions (Fig. 6) for each scenario provides further evidence of the stability of LEO population in the Normal, Maunder-like and Dalton-like scenarios: across the full projection period, the catastrophic collision rate in the Normal scenario is constant at 0.17 yr^{-1} (R^2 = 0.9984); this compares with 0.183 yr^{-1} (R^2 = 0.9992) for the period 2100 through 2209 in the Maunder-like scenario and 0.154 yr^{-1} (R^2 = 0.9999) in the Dalton-like scenario. The total number of catastrophic collisions differs between the Normal and Maunder-like scenarios by only 14.71, at the end of the projection period.

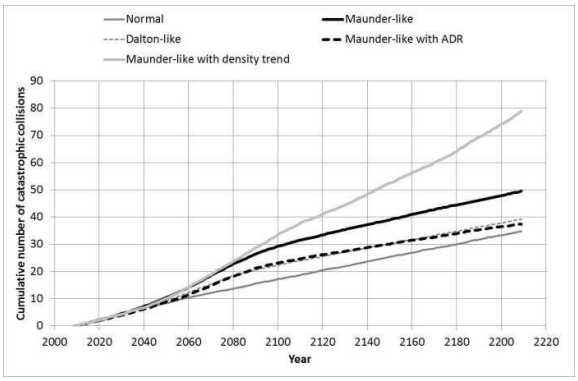

Figure 6. Cumulative number of catastrophic collisions in LEO for each DAMAGE scenario.

The collision rate is primarily determined by the number of intact objects in the LEO population and Fig. 7 shows that the difference between the number of intact objects in the Maunder-like scenario is 200 more than found in the Normal scenario shortly after year 2100, compared with a difference of 1550 in the year 2075. At the end of the projection period, the difference in the number of intact objects is less than 110 objects. The surplus objects would have otherwise re-entered under normal solar activity conditions, but their orbits continued to decay during the prolonged minimum and, hence, the objects re-enter more quickly on return to normal conditions.

Whilst the LEO population continues to grow in the Maunder-like scenario with ADR throughout the period 2020 to 2065, the remediation limits the growth to a rate of about 150 objects per year (Fig. 5). By the end of the projection period, the LEO population has increased by 2% only, compared with the initial population, in spite of the rapid increase during the prolonged solar minimum.

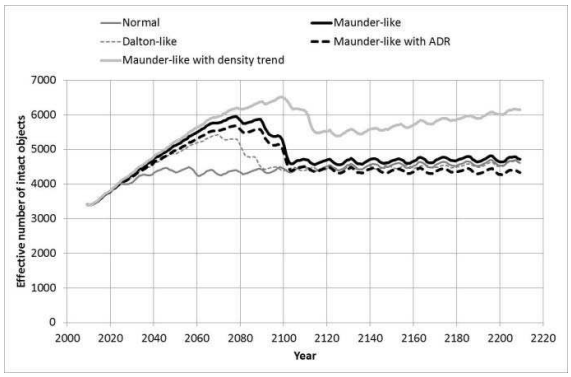

Figure 7. Effective number of intact objects≥ 10 cm in LEO, for each DAMAGE scenario.

In contrast, the LEO population in the Maunder-like scenario, with the atmospheric mass density trend, demonstrates the characteristics of an unstable system. Under these "worst-case" conditions, the LEO population shows only short-term decline during the solar maxima following the prolonged minimum, and no long-term decrease in the number of objects (Fig. 5). Here the LEO population grows by 187% by the end of the projection period, with the growth driven by an ever-increasing catastrophic collision rate (Fig. 6). 69% of these catastrophic collisions occur at altitudes at or below 800 km (Fig. 8). Similar altitude distributions are observed for the Maunder-like scenario (65%) and the Dalton-like scenario (63%), but the distribution differs for the Normal scenario, in which 57% of the catastrophic collisions occur at or below 800 km.

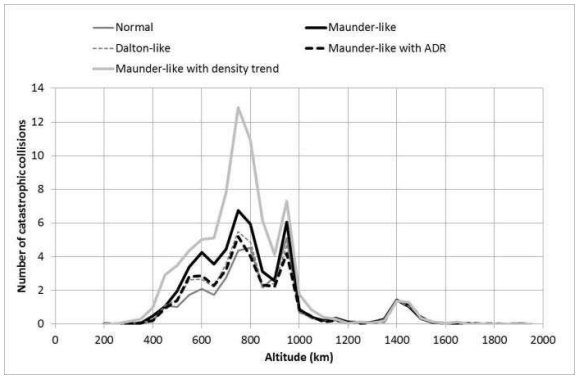

Figure 8. Number of catastrophic collisions as a function of altitude for each DAMAGE scenario.

Thus, it can be argued that the additional catastrophic collisions that would arise as a result of a prolonged solar minimum (Fig. 6; whether Maunder-like or Dalton-like) are likely to occur at lower altitudes than expected under normal solar conditions. As a result of the return to a regular solar cycle, the fragments generated by these catastrophic collisions are subject to increased drag by virtue of their lower orbits and so re-enter at an elevated rate. This hypothesis is supported by the time-history of collision fragments in Fig. 9.

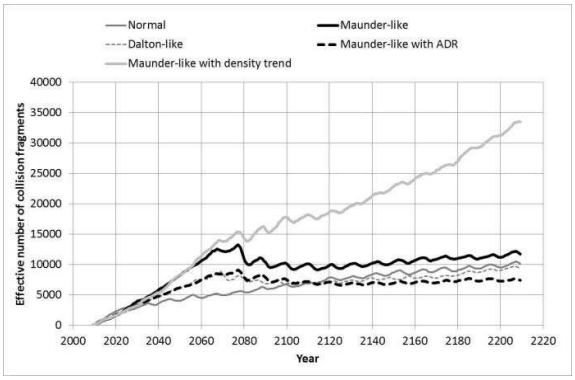

Figure 9. Effective number of collision fragments≥ 10 cm in LEO, for each DAMAGE scenario.

The addition of a secular density trend, however, disrupts the drag force and resultant re-entry process, as the mass density at the lower altitudes has undergone a decline. Consequently, the reduced rate of re-entry of intact objects (Fig. 7) and collision fragments (Fig. 9) leads to an overall increase in the LEO population, as well as to an increase in the catastrophic collision risk.

5 CONCLUSIONS

The DAMAGE results suggest that the population of debris ≥ 10 cm could double in number if the Sun enters a prolonged period of low activity, similar to the Maunder minimum or Dalton minimum. During these conditions, the benefits of space debris mitigation and remediation measures are significantly reduced. However, the rapid growth in the population is followed by a strong recovery period on exit from a Maunder-like or Dalton-like minimum. The recovery is driven by the re-entry of intact objects and collision fragments at an enhanced rate, to a level similar to that seen before the onset of the prolonged minimum, if mitigation efforts are sustained. This response is characteristic of a stable system.

If a prolonged minimum occurs in conjunction with a decline in global atmospheric mass density, the debris population may not recover to pre-minimum levels. In fact, this situation shows the traits of an unstable system with a clear runaway debris population in spite of the continued implementation of mitigation measures.

Aside from this worst-case, prolonged solar minimum conditions may have relatively benign implications for the long-term evolution of the debris environment. This prognosis can be reinforced through the adoption of remediation measures, such as Active Debris Removal. However, the risks to spacecraft from collisions with debris during a Maunder-like minimum would be considerably higher than present, and exacerbated by

any deficiency in debris mitigation efforts, with corresponding impacts on space operations.

6 ACKNOWLEDGEMENTS

The authors would like to thank Holger Krag and Heiner Klinkrad, ESA, for permission to use and assistance with the MASTER 2009 population, and Professor Sir John Beddington (Imperial College London) for continued motivation.

7 REFERENCES

1. M. Lockwood, M., Owens, M., Barnard, L., Davis, C., and Thomas, S. (2012), Solar cycle 24: what is the Sun up to?, Astron. and Geophys., v.53, 3.9.
2. Howe, R., Christensen-Dalsgaard, J., Hill, F., Komm, R., Larson, T.P., Rempel, M., Schou, J. and Thompson, M.J. (2013), The high-latitude branch of the solar torsional oscillation in the rising phase of cycle 24, Ap. J. Lett., 767:L20, doi:10.1088/2041-8205/767/1/L20.
3. Barnard, L., Lockwood, M., Hapgood, M.A., Owens, M.J., Davis, C.J., and Steinhilber, F. (2011), Predicting space climate change, Geophys. Res. Lett., v.38, L16103, doi:10.1029/2011GL048489.
4. Liou, J.-C., Hall, D.T., Krisko, P.H., and Opiela, J.N. (2004), LEGEND – A three-dimensional LEO-to-GEO debris evolutionary model, Adv. Space Res., 34, 981–986, doi:10.1016/j.asr.2003.02.027.
5. Emmert, J.T. and Picone, J.M. (2010), Climatology of globally averaged thermospheric mass density, J. Geophys. Res., 115, A09326, doi:10.1029/2010JA015298.2010.
6. Liou, J.-C. (2006), Collision activities in the future orbital debris environment, Adv. Space Res., 38, 2102–2106, doi:10.1016/j.asr.2005.06.021.
7. Akmaev, R. A., and Formichev, V.I. (2000), A model estimate of cooling in the mesosphere and lower thermosphere due to the CO2 increase over the last 3–4 decades, J. Geophys. Res., 27(14), 2113–2116.
8. Roble, R. G., and Dickinson, R.E. (1989), How will changes in carbon dioxide and methane modify the mean structure of the mesosphere and thermosphere?, J. Geophys. Res., 16(12), 1441–1444.
9. Keating, G. M., Tolson, R.H., and Bradford, M.S. (2000), Evidence of long-term global decline in the Earth's thermospheric densities apparently related to anthropogenic effects, Geophys. Res. Lett., 27, 1523–1526, doi:10.1029/2000GL003771.
10. Emmert, J. T., Picone, J.M., Lean, J.L., and Knowles, S.H. (2004), Global change in the thermosphere: Compelling evidence of a secular decrease in density, J. Geophys. Res., 109, A02301, doi:10.1029/2003JA010176.
11. Emmert, J. T., J. M. Picone, J. L. Lean, and R. R. Meier (2008), Thermospheric global average trends, 1967–2007, derived from orbits of 5000 near-Earth objects, Geophys. Res. Lett., 35, L05101, doi:10.1029/2007GL032809.
12. Saunders, A., Lewis, H.G., and Swinerd, G.G. (2011), Further evidence of long-term thermospheric density chance using a new method of satellite ballistic coefficient estimation, J. Geophys. Res., 116, DOI: 10.1029/2010JA016358.
13. Lewis, H. G., Swinerd, G.G., Ellis, C.S., and Martin, C.E. (2005), Response of the space debris environment to greenhouse cooling, in Proceedings of the Fourth European Conference on Space Debris, Darmstadt, Germany, 18–20 April, 2005, Eur. Space Agency Spec. Publ., ESA SP-587, 243–248.
14. Lewis, H.G., Saunders, A., Swinerd, G.G., and Newland, R.J. (2011), Effect of thermospheric contraction on remediation of the near-Earth space debris environment, J. Geophys. Res., 116, A00H08, doi:10.1029/2011JA016482.
15. Liou, J.-C., and Johnson, N.L. (2007), A sensitivity study of the effectiveness of active debris removal in LEO, paper presented at 58th International Astronautical Congress, Int. Astronaut. Fed., Hyderabad, India.
16. Johnson, N. L., Krisko, P.H., Liou, J.-C., and Anz-Meador, P.D. (2001), NASA's new breakup model of EVOLVE 4.0, Adv. Space Res., 28, 1377–1384, doi:10.1016/S0273-1177(01)00423-9.